Information on past solar activity and geomagnetism from ^{10}Be in the Camp Century ice core

J. Beer*†, U. Siegenthaler†, G. Bonani*, R. C. Finkel‡, H. Oeschger†, M. Suter* & W. Wölfli*

* Institut für Mittelenergiephysik, ETH-Hönggerberg, CH-8093 Zürich, Switzerland
† Physics Institute, University of Bern, CH-3012 Bern, Switzerland
‡ Lawrence Livermore National Laboratory, Livermore, California 94550, USA

A nearly continuous record of the concentration of ^{10}Be from ice-core data is compared with the tree-ring-derived record for ^{14}C over the same period and it is found that short-term trends in these data sets provide a record of solar activity. No definitive relationship between the long-term trends and the geomagnetic dipole moment is found.

THE radioisotope ^{10}Be, with a half-life of 1.5×10^6 yr, is continuously produced in the atmosphere by the interaction of cosmic-ray particles with nitrogen and oxygen. The radioisotope production rate depends on the atmospheric cosmic-ray flux, which varies in time owing to modulation by the solar wind or the Earth's magnetic field. After a short time ^{10}Be becomes attached to aerosols and after a mean residence time of 1–2 yr is removed from the atmosphere, mainly by precipitation. Transport and deposition are strongly dependent on atmospheric circulation and mixing processes and on the distribution and the rate of precipitation. A record of the ^{10}Be concentration in precipitation therefore potentially contains information on the history of solar activity, geomagnetic field intensity and climate.

Variations of the radioisotope production rate (and therefore of the solar and terrestrial magnetic fields) have been much discussed with reference to the tree-ring record of atmospheric ^{14}C concentration[1–3]. The geochemical behaviour of ^{10}Be is different from that of ^{14}C (^{14}C is also produced by cosmic rays in the atmosphere); in particular, ^{10}Be reflects variations in production rate much more directly than ^{14}C. On the other hand, ^{10}Be is influenced by local atmospheric processes whereas $^{14}CO_2$ is homogenously distributed in the atmosphere, so that much may be learned from a comparison of the distribution of the two stages.

Accelerator mass spectrometry (AMS) allowed measurements to be made on relatively small samples so as to reconstruct the ^{10}Be fallout history from samples of polar ice where precipitation is preserved in a stratigraphically undisturbed way.

Several studies[4–6,8–10] have already demonstrated the usefulness of ^{10}Be measurements in ice cores. At the Glacial/Holocene transition and during the last glaciation, strong variations of the ^{10}Be concentration in polar ice have been observed which are probably mainly due to changes in the precipitation rate[4–6]. Measurements at the Milcent station in central Greenland have shown that during the period of solar quiescence known as the Maunder Minimum (AD 1645–1715)[7], a period when almost no sunspots were observed, the ^{10}Be concentration was substantially higher than during other periods[8]. It appears that the 11-yr Schwabe solar cycle can also be detected in the same data[9]. First results from the Camp Century ice core, Greenland, covering the past 4,500 years have already been published[10]. We now describe variations from the same core during the past 10,000 years.

Experimental procedure

At Camp Century (north Greenland, 77°10′ N, 82° 08′ W), a 1,370-m-long ice core was drilled through the ice sheet down to the bedrock[11], covering the last glaciation back to ~100,000 years[12]. A continuous strip was cut from the core, divided into samples usually of 6 m in length and ~2 kg in mass. At two depth intervals, the Maunder Minimum (AD 1645–1715) and the Glacial/Postglacial transition (11,000 yr BP), the sampling interval was reduced to increase resolution. Samples of ^{10}Be were prepared as described previously[13] and measured using the accelerator mass spectrometer at ETH Zürich[14]. Each sample was measured at least twice, resulting in a precision of 4–10%. To have the δ^{18}O values for the very same depth intervals as ^{10}Be and to compare them with the detailed record of Dansgaard and co-workers[12], δ^{18}O was measured on aliquots of each sample.

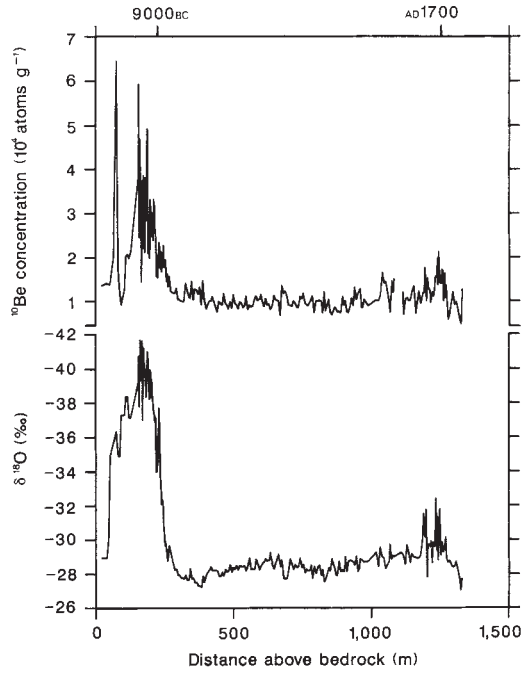

Fig. 1 ^{10}Be concentration (10^4 atoms g^{-1}) and δ^{18}O (‰) of the Camp Century ice core. The strong change of both curves at ~200 m represents the transition into the last glaciation (9000 BC). The gap in the ^{10}Be curve at ~1,100 m is caused by four missing data points. δ^{18}O is the deviation, in parts per thousand, of the ^{18}O/^{16}O ratio.

Results

Figure 1 shows the ^{10}Be concentration plotted together with δ^{18}O as a function of height above bedrock. The ^{10}Be values of the top 900 m correspond to those published earlier from Camp Century[10] except for an increase by 20% due to a recalibration of the used standard[38]. Both curves show a dramatic change at 250 m above bedrock, corresponding to the Glacial/Holocene

transition. During glacial times, the ^{10}Be concentration is considerably greater than during the Holocene and exhibits strong fluctuations which parallel the variations of δ^{18}O. Similar results obtained earlier on ice cores from Antarctica[4,6,15] and from Greenland[5] have been attributed to changes of accumulation rate[16]. During the Holocene, the fluctuations of the two curves are independent except for the range of 1,200–1,250 m corresponding to the Maunder Minimum period. Here we discuss only the Holocene part of the record. First, a timescale is established, to be used to compare the ^{10}Be record with the ^{14}C data curve deduced from measurements on tree rings.

Timescale

To determine the depth–age relation of ice cores we used an ice flow model[17] which uses two parameters (annual layer thickness, depth of vertical strain rate change) that are not precisely known. To allow for this, two reference depths of known ages were taken (Fig. 1). (Because the core drilling did not begin at the surface, the top of the core is not a well-defined reference point.) We have, however, been able to identify the Maunder Minimum by correlating the Camp Century ^{10}Be record with that of Milcent, which has been dated using seasonal δ^{18}O variations (see ref. 10, Fig. 2). The estimated dating accuracy is ±20 yr. As a second reference point, we took the steep δ^{18}O increase at 1,133 m depth, already identified as the end of the Younger Dryas cold phase in Europe with a conventional ^{14}C age of 10,000 ± 200 yr BP[19] using a correlation with oxygen isotope records from lake sediments[18]. For the absolute age we have to correct for variations of the atmospheric ^{14}C concentration. Extrapolating backwards the tree-ring ^{14}C series[20], which date back to ~9,000 yr BP, we estimate $\Delta^{14}C = 90 \pm 30‰$ at the end of the Younger Dryas, which corresponds to results obtained from Swedish varves[21]. This leads to an absolute age of 9,050 ± 300 BC (11,000 ± 300 yr BP) for our second reference point, consistent with the result of Hammer *et al.*[22] based on counting annual dust layers. The two parameters of the ice flow model were then tuned to fit the fixed points.

In Fig. 2, ^{10}Be is plotted against the resulting absolute age for the past 10,000 years (Holocene). In addition to the data from Camp Century, the results from Milcent, Greenland, covering the time AD 1180–1800 (ref. 8), have also been included after adjustment to both the depth–age scale and the mean ^{10}Be value of the Camp Century data for the same time span. Because of the thinning of the annual layers with depth, the lower (older) part of the curve is significantly expanded compared to Fig. 1.

Comparison of ^{10}Be and ^{14}C records

The Holocene ^{10}Be record in Fig. 2 shows significant variations on long timescales (for example, maxima between 6000 and 4000 BC and after AD 1000) as well as on timescales of centuries. The question is whether the observed variations are caused by changes in climate or changes of the radioisotope production rate. The ^{10}Be decrease before 7000 BC coincides with a δ^{18}O increase (see Fig. 1) and may be due to climate effects; perhaps the north Greenland ice sheet was still adapting to the transition from Glacial to Holocene conditions. After 7000 BC, there is no clear correlation between ^{10}Be and δ^{18}O (except for the range 1,200–1,250 m which corresponds to the Maunder Minimum period), suggesting that short-term ^{10}Be fluctuations are mainly caused by changes of the production rate and not by climate effects.

To test this hypothesis we have compared our results with the Δ^{14}C record from tree-ring measurements[20] (Fig. 3*b*). (Δ^{14}C is the deviation, in parts per thousand, of the ^{14}C concentration from a standard value. Around AD 1800, atmospheric Δ^{14}C was ~0‰.) The production of both ^{10}Be and ^{14}C by cosmic rays in the atmosphere depends on the energy spectrum of the primary particles. Changes of the cosmic-ray flux due to solar and geomagnetic modulation therefore cause variations of production rate of comparable relative amplitude[23]. If the observed ^{10}Be fluctuations are due to changes of production rate, then similar variations should have occurred in the ^{14}C record, but if climate effects are responsible, the two records should be uncorrelated. ^{10}Be is scavenged from the atmosphere within one or two years of its creation; production rate changes are therefore reflected in the ice directly, without attenuation. By contrast, ^{14}C, present in the form of CO_2, is first diluted by the atmospheric CO_2 mass and, with time, by increasing contributions from the other carbon pools, ocean and biosphere. The atmospheric ^{14}C concentration therefore reflects high-frequency variations of the production rate only with strong attenuation; on the other hand, it preserves a memory of previous production-rate changes. Thus, the global carbon exchange system acts as a low-pass filter for the ^{14}C production variations[24].

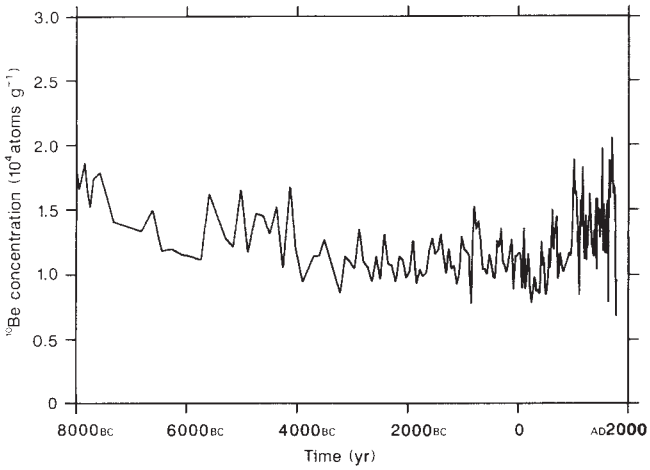

Fig. 2 ^{10}Be concentration of Fig. 1 plotted against time for the upper 1,000 m. For the period AD 1180–1800 the results from Milcent (central Greenland)[8] are also included after corresponding adjustments of the depth–age scale and the mean value.

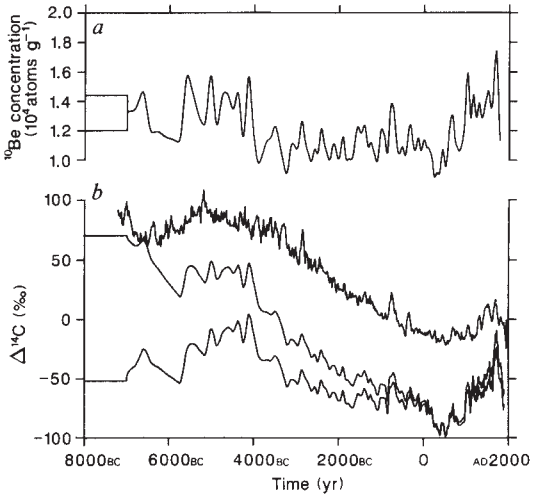

Fig. 3 *a*, ^{10}Be concentration of Fig. 2 from 7000 BC onwards, used as input function for the model calculations (units: 10^4 atoms g^{-1}). The data were slightly smoothed. The two straight lines before 7000 BC represent the two initial conditions (1.20×10^4 and 1.44×10^4 atoms g^{-1}). *b*, Measured atmospheric Δ^{14}C data[20] from tree rings and calculated Δ^{14}C data using the ^{10}Be data of *a* as input to the box-diffusion model. The calculations were carried out for the two different initial conditions as indicated in Fig. 3*a*. The resulting model curves were shifted by 70‰ for an easier comparison with the measured Δ^{14}C data.

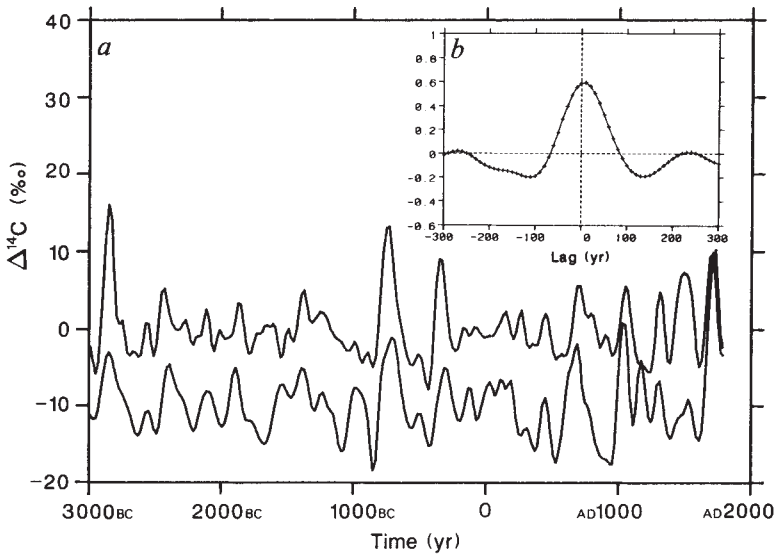

Fig. 4 *a*, Enlargement of the period 3000 BC to AD 2000 of Fig. 3*b* after removal of the long-term trends by a high-pass filter. The upper curve represents the measured $\Delta^{14}C$ variations[20]; the lower shows calculated $\Delta^{14}C$ based on the ^{10}Be data using the higher initial conditions of Fig. 3*a*. The lower curve is shifted by 10‰ for easier comparison. Both curves are slightly smoothed. *b*, Cross-correlation coefficient between the measured and calculated $\Delta^{14}C$ curves (see *a*) as a function of lag time.

To compare the ice-core ^{10}Be record and the tree-ring ^{14}C data, we have simulated the low-pass filtering effect of the exchange system by means of an appropriate carbon cycle model. The model used is a modified version[25] of the original box-diffusion model of Oeschger *et al.*[26]. The atmosphere is subdivided into stratosphere and troposphere, and a four-box terrestrial biosphere is included. The ocean is treated as a diffusive medium. The dynamic ocean model parameters are derived from the natural distribution of ^{14}C (ref. 27).

We assume for simplicity that the effects of atmospheric transport and mixing processes can be neglected and therefore that the ^{10}Be concentration in the Camp Century samples is directly proportional to the global production rate of ^{10}Be as well as to that of ^{14}C. Thus we use the ^{10}Be concentration record (Fig. 3*a*) as the model input function for describing the relative variations of the atmospheric ^{14}C production rate after 7000 BC. For the model results, the value of the standard ^{14}C concentration is a free parameter and is chosen such that for the period AD 0–1000 the calculated average $\Delta^{14}C$ agrees with the tree-ring mean of −14.6‰. The simulation is started in 7000 BC, a time when the ^{10}Be values at Camp Century seem to be no longer influenced by the Glacial/Holocene transition. Due to the long memory of the ^{14}C system, the long-term behaviour of the calculated ^{14}C concentration is strongly dependent on the production-rate history before the start-time of the model. At the end of the last glaciation and in the early Holocene the ^{10}Be signal was strongly dominated by climate effects, and therefore the detailed isotope production rate history before 7000 BC is difficult to derive from the Camp Century record. For the calculations, we first assume that the production rate is constant before 7000 BC, with a value corresponding to the mean ^{10}Be concentration during the period 7000 BC to AD 1800 (1.20×10^4 atoms g^{-1}). The calculations were repeated for an initial production rate higher by 20%. As seen in Fig. 3*b*, this second curve fits the actual long-term $\Delta^{14}C$ trend relatively well.

Short-term variations

Short-term variations of the atmospheric ^{14}C concentration are known to have occurred fairly regularly. High-precision tree-ring measurements[20] have clearly confirmed the existence of fluctuations of ~200-yr duration and a peak-to-peak amplitude of ~20‰ ('Suess wiggles')[2,28–30], as seen in Fig. 3*b*. ^{10}Be fluctuations on a similar timescale are observed, with much larger amplitude, typically ~40%. We wish to demonstrate that these variations are caused by changes in production rate.

To test this hypothesis, we compare model-generated ^{14}C variations with the tree-ring data of the period 3000 BC to AD 1800, an interval where the time resolution of the ^{10}Be record is good. The long-term trend was removed from both curves by applying a binomial high-pass filter. The resulting curves (Fig. 4*a*), are very similar; for example, the prominent maxima of the tree-ring record at ~2800 BC, 1900 BC, 700 BC, 300 BC, AD 800, AD 1100 and AD 1700 (Maunder Minimum) are also found in the ^{10}Be-based model curve.

A quantitative measure of the similarity between the two curves is obtained using the cross-correlation function (Fig. 4*b*). The correlation coefficient has a clear maximum for a shift near zero; its value of 0.58 differs from zero with very high significance ($P > 0.999$), and the amplitudes of the variations for the two curves agree well (Fig. 4*a*). The standard deviation is 3.9‰ for the tree-ring data and 4.4‰ for the model-calculated time series. All this is strong evidence that the isotope variations have a common cause, namely changes in production rate.

^{14}C variations over the past centuries are well correlated with sunspot numbers, which indicates that the short-term variations are probably due to a changing Sun[3]. During the Maunder Minimum, solar activity was considerably reduced, as indicated by very low numbers of observed sunspots and aurorae[7], and consequently the solar wind was reduced. This was presumably also the case during the other periods of isotope concentration maxima.

We have limited this comparison to the time since 3000 BC, because before that the time resolution of the ^{10}Be record, which becomes coarser with increasing age, is not sufficient to resolve fluctuations of 200-yr duration. Indeed, the wiggles of the tree-ring $\Delta^{14}C$ curve before 3000 BC are not simulated well by the ^{10}Be-based model curve (Fig. 3*b*).

A by-product of the comparison is that the timescale constructed for the Camp Century ice core seems to be accurate, at least for the period from 3000 BC to the present.

Could the short-term isotope variations be related to climatic variability? Variations in snowfall rate can cause varying ^{10}Be concentration in polar ice. For Milcent station, we estimated the annual accumulation for the time span AD 1180–1800 based on the detailed $\delta^{18}O$ profile of Dansgaard *et al.* (S. Johnsen, personal communication), and found that it varies by ~10%. The calculated ^{10}Be flux exhibits the same pattern of variation as the ^{10}Be concentration at this station; no systematic difference can be seen between flux and concentration. For the Camp Century core, a detailed history of the accumulation rate is not available, and the only parameter that can possibly give any information on climate-induced ^{10}Be variations is $\delta^{18}O$. To see whether the observed ^{10}Be variations might be connected to climatic changes, we applied a correction, based on the assumption of an inverse proportionality between concentration and accumulation rate[6]. (A change of 1‰ in $\delta^{18}O$ corresponds to a

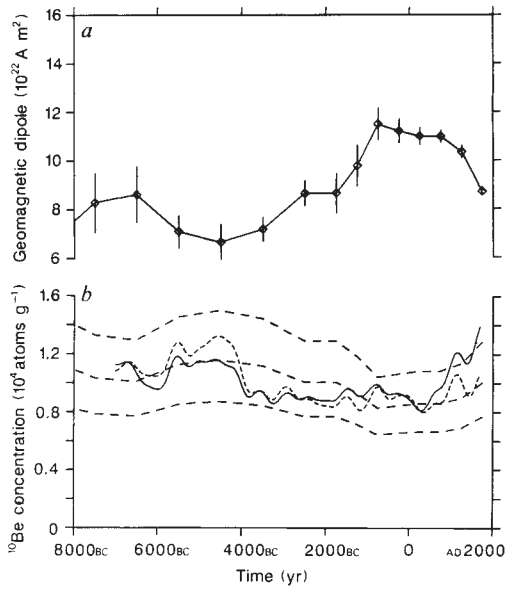

Fig. 5 *a*, Geomagnetic dipole moment M in units of 10^{22} A m^2 as derived from palaeomagnetic data[33]. *b*, Smoothed measured ^{10}Be concentration (solid line) according to Fig. 2 and δ^{18}O-corrected ^{10}Be concentrations (dotted line). Both curves are normalized to the mean value of 1. The three dashed curves represent the expected ^{10}Be production according to the palaeomagnetic data (*a*) for three levels of solar activity (low, normal, high)[23].

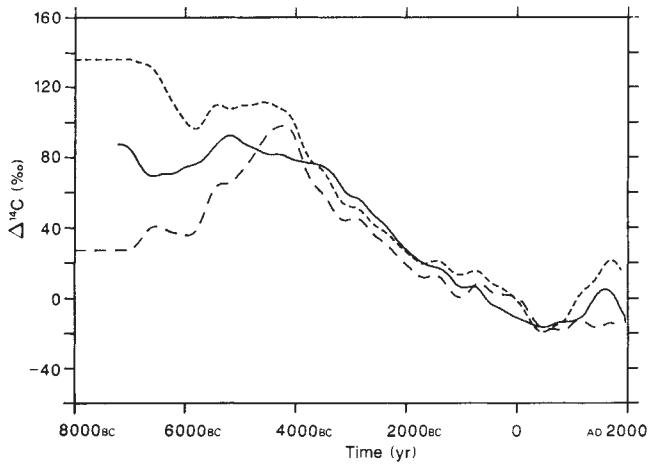

Fig. 6 Comparison of the long-term Δ^{14}C trends. Solid line, Δ^{14}C variations measured in tree rings[20]; dotted lines, calculated Δ^{14}C variations based on the original (upper) and the δ^{18}O-corrected (lower) ^{10}Be data.

20% change in ^{10}Be.) As a result, the amplitude of some of the short-term ^{10}Be fluctuations are altered, but generally, the δ^{18}O correction has a small effect. These results therefore indicate that climatic effects (at least those reflected in δ^{18}O), are not the main cause of short-term ^{10}Be variations during the Holocene.

Long-term variations

The ^{10}Be record also exhibits changes on timescales of >1,000 yr (Fig. 2). Concentrations from ~6000 to 4000 BC and after AD 500 were ~20% higher than in the between period. These changes cannot be explained by climatic influences as expressed in δ^{18}O variations, because the δ^{18}O correction does not decrease the overall variability.

The long-term trend of the Δ^{14}C curve has often been attributed to variations of the geomagnetic dipole moment[1,31] using the equation[32] $Q/Q_0 = (M/M_0)^{-0.5}$ for the relation between isotope production rate Q and dipole moment M (Q_0 and M_0 denote present-day values). Figure 5*a* shows a compilation of a large number of palaeomagnetic data[33]. These data, especially those from older periods, are subject to considerable uncertainty, as they are partly based on measurements from only a few regions and may reflect local non-dipole fields[34]. In Fig. 5*b*, the smoothed ^{10}Be data are plotted together with the production rate calculated for the geomagnetic intensity of Fig. 5*a*, for three levels of solar activity (low, normal, high)[23]. The calculated trend for constant normal solar activity shows rather poor agreement with the uncorrected ^{10}Be data (solid line). The δ^{18}O-corrected curve (dashed line) agrees better with the calculated curve.

Thus, the observed variations and those expected from palaeomagnetic data are not in good agreement, as already found earlier[10]. But the production rate in high latitudes is not predominantly modulated by geomagnetic field variations, so that a high-latitude record, which to some extent reflects locally produced ^{10}Be, is not ideal for studying dipole moment variations. On the other hand, a reconstruction of the geomagnetic field intensity is not without problems, so that the data in Fig. 5*a* are subject to some uncertainty[34].

Figure 6 shows the (smoothed) model Δ^{14}C curves for the original and the δ^{18}O-corrected ^{10}Be data, both for a pre-7000 BC ^{10}Be concentration of 1.44×10^4 atoms g^{-1}. Although the decrease from 4000 BC to AD 500 is similar, there are clear differences before 4000 BC and after AD 500. The curve obtained from the δ^{18}O-corrected ^{10}Be data does not simulate the tree-ring record as well for these periods, and therefore does not support making the δ^{18}O correction on the ^{10}Be record.

When discussing the long-term trend it is important to be aware that the ^{14}C system has a long memory; the model-simulated trends (Figs 3, 6) depend strongly on the initial conditions. For a pre-7000 BC production rate higher by 20% (upper curve in Fig. 3*b*), the long-term tree-ring trend is relatively well simulated. This means that the decreasing trend does not necessarily imply a slowly decreasing production rate after 4000 BC, but could well be the consequence of ~20% higher production rate before 7000 BC. Because the global ^{14}C inventory adjusts to long-term production rate changes with a half-life of 5,730 yr, a new quasi-steady state would not be reached yet. Therefore the mean pre-7000 BC ^{14}C concentration would not have been +200‰, but ~+140‰. (Note that 0‰ corresponds to the atmospheric value at ~AD 1800.)

It has been thought that the long-term ^{14}C trend might be caused by a gradual increase in the speed of ocean circulation[35], which leads to a faster vertical ocean circulation and therefore to an increased release of 'old', ^{14}C-depleted CO_2 into the atmosphere[24]. Simultaneous ^{14}C measurements on surface-dwelling and bottom-dwelling foraminifera[36] on a deep-sea sediment core do not support the suggested speed-up of the circulation. It seems, however, well established that during glacial time the rate of deep-water formation in the North Atlantic was reduced, which must have caused higher atmospheric ^{14}C concentrations by ~50–100‰. A model simulation[25] indicates that the atmospheric ^{14}C concentration adapts within <1,000 yr to a change towards a faster ocean circulation such as that which occurred ~13,000 years ago. This, and the foraminiferal ^{14}C data, show that the long-term Δ^{14}C trend cannot be an after-effect of an internal change in the carbon system at the end of glacial time.

Although no final conclusions can be drawn regarding the origin of the Δ^{14}C long-term trend, the available information is sufficient to advance a hypothesis different from the often discussed picture[1,31] that this trend is the direct result of changing geomagnetic dipole moment. The comparison of ^{10}Be and ^{14}C suggests that the isotope production rate was higher by 20% during the last 10,000–15,000 yr of the ice age, leading to correspondingly higher ^{14}C concentrations in all carbon reservoirs

($\Delta^{14}C = 140‰$ in the atmosphere). If the production rate changed to the present-day value some time in the early Holocene, the decreasing trend between 5000 and 0 BC would reflect the exponential decay of ^{14}C with a half-life of 5,730 yr. The maximum of the ^{14}C concentration between 6000 and 4000 BC and the increase after AD 0 could have been caused by a changing geomagnetic dipole moment, as indicated by the palaeomagnetic data[33].

The late glacial production rate is therefore essential for the interpretation of the long-term trend in ^{14}C concentration. Unfortunately, the ^{10}Be signal at that time is completely masked by climate effects. There are, however, ^{14}C dates from varves[21] indicating that the atmospheric ^{14}C level was higher at the end of the last glaciation. These results are in agreement with data indicating that the geomagnetic field was weaker during the period 50,000–10,000 yr BP[37].

Conclusions

The comparison of the Camp Century ^{10}Be record with $\delta^{18}O$ and $\Delta^{14}C$ shows that ^{10}Be measurements on polar ice cores give valuable information. Strong climatic changes such as the transition from glacial to interglacial times or climatic fluctuations during glaciation are clearly visible in the ^{10}Be record, but climatic variations do not seem to have had much influence during the Holocene. The good correlation between the main short-term variations of both the ^{10}Be record in ice and the ^{14}C record in tree-rings over the past 5,000 yr strongly supports the explanation that these fluctuations are caused by solar modulation of the Galactic cosmic-ray flux. The comparison of ^{10}Be and ^{14}C also makes possible the refinement of ice-core dating using the technique of wiggle matching.

Less clear conclusions can be drawn regarding the long-term isotope variations. The ^{10}Be data do not give support to the hypothesis that the observed slow ^{14}C decrease was due to a gradual geomagnetic field change. They suggest, rather, that the ^{14}C trend might be the result of a 20% higher production rate during the last 10,000–15,000 years of the ice age.

We thank C. C. Langway, B. Kapuza and M. Andrée for help with the ice sampling, K. Hänni for measuring $\delta^{18}O$, H. J. Hofmann, E. Morenzoni and M. Nessi for help during the ^{10}Be measurements and C. U. Hammer, H. Clausen and B. Stauffer for useful discussions. This work was supported financially by the Swiss NSF.

Received 20 July; accepted 7 December 1987.

1. Bucha, V. in *Radiocarbon Variations and Absolute Chronology*, 501-513 (Almquist & Wiksell, Stockholm, 1970).
2. Suess, H. in *Radiocarbon Variations and Absolute Chronology*, 595-605 (Almquist & Wiksell, Stockholm, 1970).
3. Stuiver, M. & Quay, P. D. *Science* **207**, 11-19 (1980).
4. Raisbeck, G. M. *et al. Nature* **292**, 825-826 (1981).
5. Beer, J. *et al. Ann. Glaciol.* **5**, 16-18 (1984).
6. Yiou, F., Raisbeck, G. M., Bourles, D., Lorius, C. & Barkov, N. I. *Nature* **316**, 616-617 (1985).
7. Eddy, J. A. *Science* **192**, 1189-1201 (1976).
8. Beer, J. *et al.* in *Proc. 18th int. Cosmic Ray Conf. Bangalore* vol. 9 (eds Durgaprasad, N., Ramadurai, S., Ramana Murthy, P. V., Rao, M. V. S. & Sivaprasad, K.) 317-320 (P. V. Ramana Murthy, Bombay, 1983).
9. Beer, J. *et al. Nucl. Instrum. Meth.* **B10/11**, 415-418 (1985).
10. Beer, J. *et al. Nucl. Instrum. Meth.* **B5**, 380-384 (1984).
11. Ueda, H. T. & Garfield, D. E. *U.S. Army Cold Regions Res. Engng Lab. spec. Rep.* 126 (1968).
12. Johnsen, S. J., Dansgaard, W., Clausen, H. B. & Langway, C. C. *Nature* **235**, 429-434 (1972).
13. Beer, J. *et al. Radiocarbon* **25**, 269-278 (1983).
14. Suter, M. *et al. Nucl. Instrum. Meth.* **B5**, 117-122 (1984).
15. Raisbeck, G. M. *et al. Nature* **326**, 273-277 (1987).
16. Raisbeck, G. M. & Yiou, F. *Ann. Glaciol.* **7**, 138-140 (1985).
17. Hammer, C. U. *et al. J. Glaciol.* **20**, 3-25 (1978).
18. Oeschger, H. *et al. Geophys. Monogr.* **29**, 299-306 (1984).
19. Mangerud, J., Andersen, S. T., Berglund, B. E. & Donner, J. J. *Boreas* **3**, 109-128 (1974).
20. Stuiver, M. & Kra, R. S. *Radiocarbon* **28**, 805-1016 (1986).
21. Stuiver, M., Kromer, B., Becker, B. & Ferguson, C. W. *Radiocarbon* **28**, 969-979 (1986).
22. Hammer, C. U., Clausen, H. B. & Tauber, H. *Radiocarbon* **28**, 284-291 (1986).
23. Blinov, A. *Proc. NATO adv. Res. Workshop* Durham, 1987 (eds Stephenson, R., Wolfendale, A. & Eddy, J. A.) (Reidel, Dordrecht, in the press).
24. Siegenthaler, U., Heimann, M. & Oeschger, H. *Radiocarbon* **22**, 177-191 (1980).
25. Siegenthaler, U. & Beer, J. *Proc. NATO adv. Res. Workshop* Durham 1987 (eds Stephenson, R., Wolfendale, A. & Eddy, J. A.) (Reidel, Dordrecht, in the press).
26. Oeschger, H., Siegenthaler, U., Gugelmann, A. & Schotterer, U. *Tellus* **27**, 168-192 (1975).
27. Siegenthaler, U. *J. geophys. Res.* **88**, 3599-3608 (1983).
28. Damon, P. E., Lermann, J. C. & Long, A. *A. Rev. Earth planet. Sci.* 6457-6494 (1978).
29. Neftel, A., Oeschger, H. & Suess, H. *Earth planet. Sci. Lett.* **56**, 127-147 (1981).
30. Sonett, C. P. *Rev. Geophys. Space Phys.* **22**, 239-254 (1984).
31. Damon, P. E. & Linick, T. W. *Radiocarbon* **28**, 266-278 (1986).
32. Elsasser, W., Ney, E. P. & Winckler, J. R. *Nature* **178**, 1226-1227 (1956).
33. McElhinny, M. W. & Senanayake, W. E. *J. Geomagn. Geoelectr.* **34**, 39-51 (1982).
34. Barton, C. E., Merrill, R. T. & Barbetti, M. *Phys. Earth planet. Inter.* **20**, 96-110 (1979).
35. Lal, D. *Geophys. Monogr.* **32**, 221-233 (1985).
36. Andrée, M. *et al. Clim. Dyn.* **1**, 53-62 (1986).
37. Barbetti, M. & Flude, K. *Nature* **279**, 202-205 (1979).
38. Hofmann, H. J. *et al. Nucl. Instrum. Meth.* **B29**, 32-36 (1987).

A back-propagation programmed network that simulates response properties of a subset of posterior parietal neurons

David Zipser* **& Richard A. Andersen†**

* Institute for Cognitive Science, University of California, San Diego, La Jolla, California 92093, USA
† Department of Brain and Cognitive Sciences, Massachusetts Institute of Technology, Cambridge, Massachusetts 02139, USA

Neurons in area 7a of the posterior parietal cortex of monkeys respond to both the retinal location of a visual stimulus and the position of the eyes and by combining these signals represent the spatial location of external objects. A neural network model, programmed using back-propagation learning, can decode this spatial information from area 7a neurons and accounts for their observed response properties.

THIS article addresses the question of how the brain carries out computations such as coordinate transformations which translate sensory inputs to motor outputs. Visual inputs are collected in the coordinate frame of the retina on which the visual environment is imaged, but motor movements such as reaching are made to locations in external space. Changes in eye position will alter the retinal locations of targets while their spatial locations remain constant. As a result, visual inputs must be transformed from retinal coordinates to coordinates that specify the location of visual objects with respect to the body to perform accurately directed movements.

Lesions to the posterior parietal cortex in monkeys and humans produce profound spatial deficits in both motor behaviour and perception[1-5]. Humans with lesions to this area can still see but they appear to be unable to integrate the position of their bodies with respect to visual inputs. The lesion data further suggest that it is the inferior parietal lobule, which comprises the posterior half of the posterior parietal cortex,